

# Intersystem crossing in oligothiophenes studied by fs time-resolved spectroscopy

W. Paa, J.-P. Yang, S. Rentsch\*

Institute for Optics and Quantum Electronics, Friedrich-Schiller-University Jena, Max-Wien-Platz 1, 07743 Jena, Germany

Received: 6 December 1999/Published online: 2 August 2000 – © Springer-Verlag 2000

**Abstract.** High triplet quantum yields of more than 90% for bithiophene and terthiophene have to be connected with very fast and effective formation of triplets after excitation. We studied these processes with fs pump–probe spectroscopy. The time behaviour of transient optical spectra within the singlet and triplet manifold was examined for bi- and terthiophene (2T and 3T) in solution.

For 2T we used two-photon absorption for excitation. We found transient spectra of the excited singlet state, the triplet state and that of radical cations. The kinetics of the excited-state absorption was described by a bi-exponential function. Additionally we observed formation and recombination of radical cations. The recombination is connected with triplet formation. Both processes could be described by a time constant of  $62 \text{ ps} \pm 9 \text{ ps}$ .

For 3T we found a dependence of the processes on excitation energy using one-photon absorption. The triplet quantum yield increased with higher excitation energy. The kinetics becomes bi-exponential with increasing amplitude of the short time constant of 2 ps at increasing excitation energy.

The main reasons for the effective intersystem crossing (ISC) in both oligothiophenes are – besides the high spin-orbit coupling factor introduced by the sulphur atom – the almost isoenergetic positions of the  $S_1$  and  $T_2$  states, detected by PD-PES [1]. At higher photon excitation energy for 3T above the band gap an additional channel for ISC was detected. We believe that during the geometric change from the non-relaxed non-planar to the relaxed planar excited state  $S_1$ , ultrafast intersystem crossing takes place.

**PACS:** 42.62.Fi; 78.40.Me; 78.55.Bq; 79.47.+p

Conjugated organic polymers are of high interest because of their technical applications in molecular electronics, nonlinear optics and as organic light-emitting diodes (OLEDs). Polythiophenes are very promising because of their good processibility and high stability [2]. Oligothiophenes with  $n$  monomers per molecule, named  $nT$ , are of interest for two

reasons: (i) because of their well-defined structures they are suitable to study properties at the transition from monomer to polymer and (ii) they have their own importance as high-quality layers and films for applications [3].

Recently, derivatives of 5T were produced as high-performance OLEDs [4, 5]. The 5T derivatives show, as a powder, a fluorescence quantum yield of 37%, which is similar to the value in solution [6]. Progress was achieved in the efficiency of electroluminescence of the OLEDs, which amounts to 10%, a value comparable to or even better than that obtained with the well-known organic materials like PPV [7]. The optical properties of oligothiophenes are of importance for the different fields of their applications. Therefore the dependence of optical features on molecular size was studied in detail during recent years.

The optical spectra shift with size from the UV region, 303 nm for 2T, to the visible, 436 nm for 6T, indicating the increasing conjugation length of the longer oligothiophenes. The absorption spectra of  $nT$  in solution at room temperature show a broad structureless band shape, whereas the fluorescence spectra exhibit well-defined band structures. The absorption bands are a superposition of the absorption of different non-planar conformers with small energy differences ( $\Delta E < kT$ ). In contrast, the excited state  $S_1$  undergoes a geometrical relaxation to a planar molecule with quinoid-like structure, resulting in a structured emission band [8]. The fluorescence quantum yield is extremely low for 2T (0.014) and 3T (0.04), increases to 0.36 for 5T, but decreases at higher  $nT$  [8]. The fluorescence lifetime increases from about 30 ps for 2T to 900 ps for 6T [6]. The triplet quantum yield has the highest value at 2T (0.99) and decreases with 3T (0.95), 4T (0.73), 5T (0.59). At higher  $nT$  it seems to remain constant. All values are valid for benzene; in other solvents the quantum yields are found to be slightly different [3, 8]; for the systems studied in this paper they amount to 0.93 for 3T in dioxane and nearly 1.0 for 2T [8]. That means that the most important radiationless process in oligothiophenes is intersystem crossing (ISC).

Intersystem crossing is determined by three factors: (i) the spin-orbit coupling factor, (ii) the overlap which contains the energy difference of the corresponding singlet and triplet

\*Corresponding author. (E-mail: rentsch@ioq.physik.uni-jena.de)

states in the denominator and the Franck–Condon integral and (iii) the density of states of the terminal state. In oligothiophenes the spin-orbit coupling factor of the sulphur atom dominates, which is contained in each thiophene ring. But it cannot explain the decrease of triplet quantum yield with increasing oligomer size.

We clarified the size dependence of the triplet quantum yield by measuring the energy position of the triplet states relative to the singlet states by photo-detachment photoelectron spectroscopy (PD-PES) [1]. The determination of the energy of the triplet states  $T_1$  and  $T_2$  by means of PD-PES showed that in the case of 2T the state  $T_2$  has almost the same energy as  $S_1$ , in the case of 3T the state  $T_2$  is somewhat higher than  $S_1$ , while for 4T the state  $T_2$  is clearly higher. We see that the energy difference of the corresponding states determines essentially the triplet quantum yield. The decreasing triplet quantum yield with oligomer size is caused by the decreasing overlap factor.

The aim of our studies reported in this paper was to elucidate the kinetics of intersystem crossing of the small oligothiophenes 2T and 3T by measuring transient spectra. We hoped to find detailed insight into this process. Studies of 3T have shown a bi-exponential decay with an unexpected fast component, which was concluded to be connected with fast intersystem crossing. The second component correlated with the fluorescence lifetime [9]. In this paper we further confirmed this opinion by time-resolved spectra and studied the kinetics of 3T in dependence on excitation wavelengths. Additionally we performed fs spectroscopy of 2T using two-photon excitation.

## 1 Experimental

The samples of  $\alpha$ -bithiophene (2, 2'-bithiophene; cf. inset in Fig. 1) (2T) and  $\alpha$ -terthiophene (2, 2' : 5', 2''-terthiophene; cf. inset in Fig. 6) (3T) were purchased from Sigma. While 3T was used without further purification, 2T was purified by repeated recrystallization. All measurements on 3T were carried out for spectroscopic-grade dioxane solution ( $1 \times 10^{-3}$  mol/l). 2T – which was excited via two-photon absorption – was solved in ethanol ( $1 \times 10^{-1}$  mol/l) to avoid absorption and fluorescence caused by the solvent itself. The sample solution was placed in a quartz cell with optical length of 1 mm and excited at room temperature under the magic angle ( $54.7^\circ$ ) of the pump polarisation relative to the probe polarisation.

Transient transmission-change studies were performed using femtosecond pump–probe equipment. The laser source was a home-built Ti:sapphire laser system with chirped pulse amplification, which is described elsewhere [9]. For the present experiments we chose a repetition rate of 2 Hz and tuned the wavelength from 740 nm up to 820 nm. Pulse duration was measured to amount to less than 280 fs over all wavelengths and typically to less than 200 fs. The samples were excited by pulses of the second harmonic of the fundamental beam generated in a 1-mm-thick LiB<sub>3</sub>O<sub>5</sub> crystal. The excitation wavelengths used were varied between 370 nm and 410 nm. For recording time-resolved transient spectra, we generated in a sapphire window a white-light continuum pulse which was split into two pulses by a broadband beam-

splitter. The first part probed the transient absorption  $I^{\text{ref}}$  in a volume of the sample cuvette where no molecules should be excited during the pump process.  $I^{\text{ref}}$  is used for eliminating artefacts such as stray light or reflections on the air/quartz and quartz/sample interfaces. The second part of the white-light continuum pulse  $I^{\text{test}}$  probed molecules inside a volume which could be excited by the pump beam. By measuring both with and without excitation of the sample molecules, we confirm that we only record transient absorption changes.

The resulting two spectra per probe pulse were detected simultaneously with an optical multichannel analyser (OMA).

Absorbance differences  $\Delta A$  were calculated according to:

$$\Delta A(\lambda, \Delta t) = \frac{\sum_{i=1}^n \left( \frac{I_i^{\text{test}}(\lambda, \Delta t)}{I_i^{\text{ref}}(\lambda, \Delta t)} \right)^{\text{w.e.}}}{\sum_{i=1}^n \left( \frac{I_i^{\text{test}}(\lambda, \Delta t)}{I_i^{\text{ref}}(\lambda, \Delta t)} \right)^{\text{n.e.}}} \quad (1)$$

where  $n$  denotes the number of measurements averaged, ‘w.e.’ meaning with excitation and ‘n.e.’ no excitation.

We averaged 20 pulses for each spectra within the time-dynamics measurements, resulting in an accuracy of  $5 \times 10^{-3}$ . For investigating the wavelength dependence of the ISC in 3T, we accumulated 50 pulses at two fixed delay times, at the so-called zero delay and at a delay time of 1 ns when all of the fast processes such as fluorescence and excited-state excitation (ESA) are over and the photoinduced absorption arises only from triplet–triplet absorption (TTA). At these two delay times we recorded the transient spectra of the excited singlet-state absorption around 600 nm and of the triplet–triplet absorption around 460 nm, respectively. At both time delays (zero and 1-ns delay) the overlap between the pump and probe beams on the sample was repeatedly checked by optimising the  $\Delta A$  signal. For all measurements and/or calculations where the chirp of the supercontinuum could falsify the conclusions derived from the data, we calculated the chirp of the continuum using either the data themselves or independent measurements, and corrected the  $\Delta A$  values for this artefact.

## 2 Results

### 2.1 Two-photon excitation of bithiophene (2T)

In Fig. 1 absorption, fluorescence and triplet–triplet absorption spectra of 2T are depicted. As can be seen from the absorption band vanishing at 350 nm, it is not possible to excite directly the  $S_1$  state of 2T using the second harmonic of the Ti:sapphire amplifier (370–410 nm). So we decided to use two-photon absorption for excitation. The obtained time-resolved spectra show in the examined region between 400 nm and 750 nm three clearly distinguishable absorption bands (Fig. 2). The maxima are located at 426 nm, 500 nm and 590 nm, respectively. The kinetics for these wavelengths is shown in Fig. 3 (500 nm) and Fig. 4 (426 nm and 590 nm). Using these kinetics in conjunction with Fig. 1, it is not difficult to assign the band around 426 nm to the triplet–triplet absorption (TTA) overlapped by fluorescence. The band around 500 nm has been assigned to

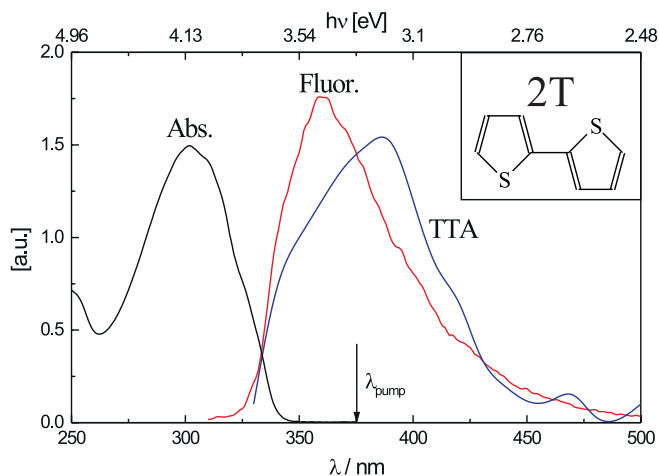


**Fig. 1.** Stationary spectra of bithiophene (2T, chemical structure shown in *inset*). Abs.: absorption, Fluor.: fluorescence, TTA: triplet-triplet absorption. Wavelength used for two-photon excitation was  $\lambda_{\text{pump}} = 375$  nm; it is marked with an arrow. Not shown is the excited-state absorption, which has its maximum at 500 nm

a  $S_1 \rightarrow S_n$  ESA [10,11]. The time behaviour at 500 nm is characterised by a bi-exponential decay with time constants of  $(29.6 \pm 4.8)$  ps and  $(1.4 \pm 0.3)$  ps (Fig. 5). The slow time constant of 29.6 ps is roughly in correspondence with the reported time constants for the ESA of  $(51 \pm 5)$  ps [10] and 40 ps [11] and indicates a reasonable fluorescence lifetime if we compare with the lifetimes of the other thiophene oligomers. The second, fast component has not yet been observed.

It is almost impossible to fit the kinetics at 426 nm with analytical functions, because of the fact that in this spectral region fluorescence and TTA strongly overlap. Furthermore we expect in this spectral region additionally a cross-correlation peak of pump and probe beams and most probably a radical absorption. Nevertheless, if we take into account only data obtained after a time delay of 70 ps, it is possible to fit the rise of the absorption with a time constant of  $(58 \pm 18)$  ps.

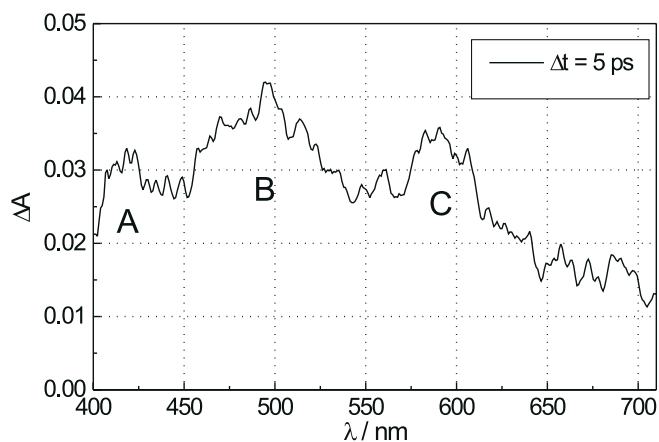


**Fig. 2.** Transient spectrum of 2T in ethanol about 5 ps after excitation with two-photon absorption. Three absorption bands attributed to ESA, TTA/fluorescence and radical cation absorption can be distinguished. The corresponding kinetics is shown in Figs. 3 and 4

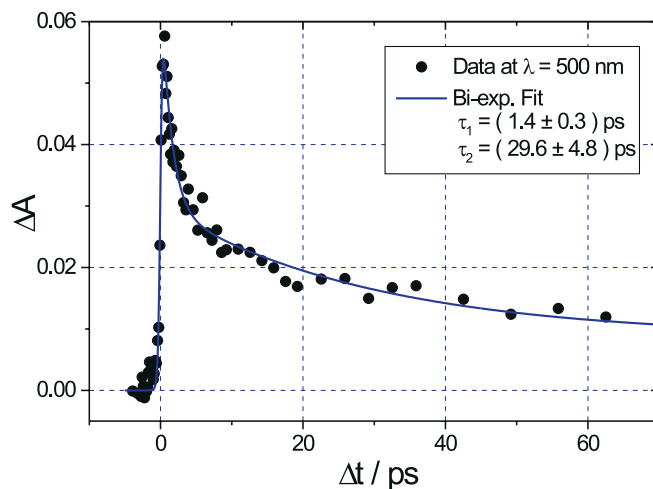


**Fig. 3.** Time dependence of  $\Delta A$  for 2T after two-photon excitation probed at a wavelength of  $\lambda = 500$  nm, where the maximum of ESA is expected. The parameters of the shown bi-exponential fit are  $\tau_1 = 1.4 \text{ ps} \pm 0.3$  and  $\tau_2 = 29.6 \text{ ps} \pm 4.8$  ps

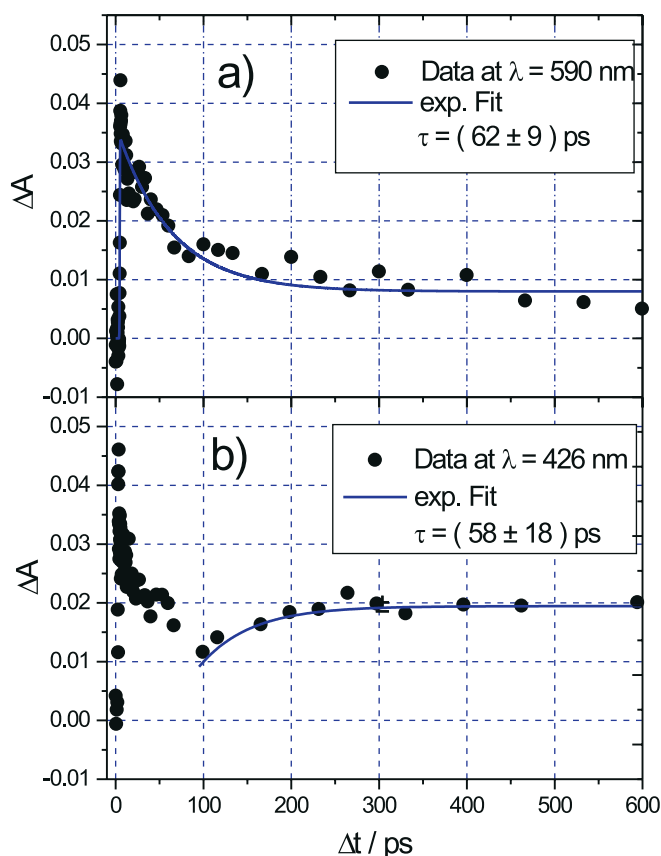


**Fig. 4a,b.** Time dependence of  $\Delta A$  for 2T after two-photon excitation probed at  $\lambda = 590$  nm (a), where a radical cation absorption band should be located, and at  $\lambda = 426$  nm (b), where TTA/fluorescence is expected. Both datasets were fitted by single exponential functions, resulting in time constants of  $62 \text{ ps} \pm 9$  ps for the radical (a) and  $58 \text{ ps} \pm 18$  ps for TTA (b)

The absorption around 590 nm has not yet been reported for 2T solved in ethanol as far as we know. Its decay can be modelled by a simple exponential function with a time constant of  $(62 \pm 9)$  ps. Despite the quite large errors, this time

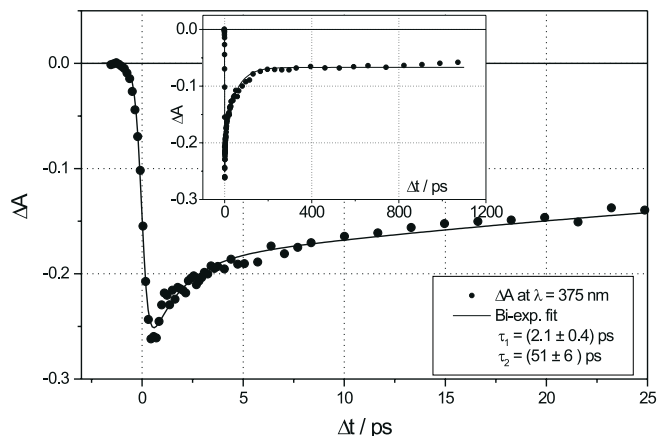


**Fig. 5.** Absorbance change in the bleaching region of 3T with  $\lambda_{\text{pump}} = \lambda_{\text{probe}} = 375$  nm. According to the rate-equation system developed in [9] the bi-exponential fit yields  $\tau_1 = 2.1 \text{ ps} \pm 0.4 \text{ ps}$  and  $\tau_2 = 51 \text{ ps} \pm 6 \text{ ps}$

constant shows a remarkable agreement with that characterising the rise of the TTA. Our interpretation is given in the Discussion.

## 2.2 Transient spectra and kinetics of terthiophene in dependence on excitation energy

Our first one-colour experiments ( $\lambda_{\text{pump}} = \lambda_{\text{probe}}$ ) in the bleaching region of 3T (Fig. 5) – reported in [9] – showed an unexpected bi-exponential decay of the bleaching with a component of 2 ps – much faster than the fluorescence lifetime of this compound (165 ps [12]) and so far unknown. This component was interpreted as a fast rise of the TTA, which overlaps partially with the fluorescing/bleaching region. As a consequence an additional second channel – situated energetically above the lowest excited singlet state  $S_1$  – for ultrafast intersystem crossing was postulated.

We tried to elucidate this result by further experiments conducted with white-light continuum for probing the transient spectra, because both spectral and time-resolved data allow us to gain a much better insight into the underlying processes of triplet formation and intersystem crossing. In Fig. 6 we show transient spectra obtained immediately after excitation (marked with 0 ps), where we see fluorescence around 430 nm and ESA around 600 nm, as well as spectra obtained 1 ns after the passage of the pump pulse. At this time delay it is justified to neglect all of the fast processes and to attribute all transients only to the TTA. Tuning the excitation energy, i.e. the wavelength of the laser, from 375 nm (Fig. 6a) to 400 nm (Fig. 6b), leads to a significant change of the ratio  $\Delta A(\text{TTA})/\Delta A(\text{ESA})$ . If we excite higher-lying singlet states within the electronic  $S_1$  manifold, the TTA increases and indicates likewise an increase of the triplet quantum yield. At energies above 3.26 eV (381 nm) however, the triplet quantum yield remains constant up to the highest energies available in our set-up. This can be seen in Fig. 7, which contains the results for all excitation energies from 3.0 up to 3.4 eV. The inset shows the relevant part of the stationary absorption spectra and (marked by arrows) the wavelengths used for excitation. Care was taken to ensure that at all wavelengths – corrected for the varying extinction coefficient – the same number of photons from the pump beam was absorbed.

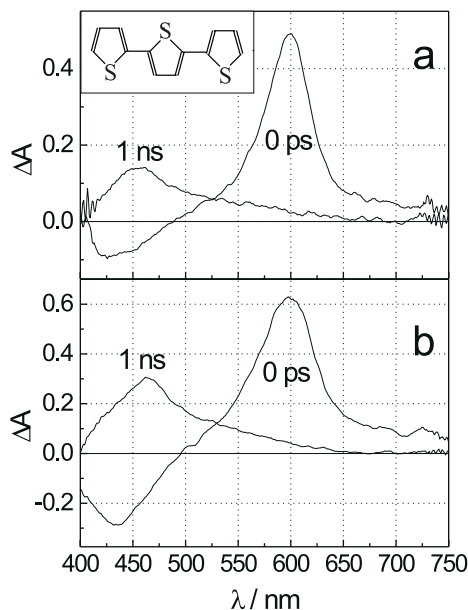


**Fig. 6a,b.** Time-resolved spectra of 3T in dioxane;  $\Delta A$  spectra at maximum of ESA (0 ps) and at a time delay of 1 ns. **a** Excitation wavelength: 400 nm; absorbed pump energy: 12.5  $\mu\text{J}$ . **b** Excitation wavelength: 375 nm; absorbed pump energy: 12.0  $\mu\text{J}$ . Inset shows the chemical structure

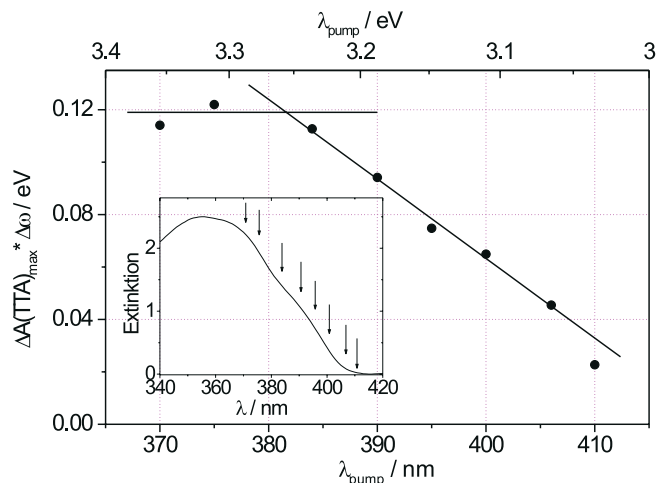


**Fig. 7.** Relative triplet generation yield for 3T at almost the same absorbed excitation photon numbers, plotted as a function of excitation wavelength. The crossing point of the two solid lines corresponds to energy of the intermediate state (see text). The inset shows the relevant part of the absorption spectrum of 3T; arrows show the wavelengths used for excitation

If the above-mentioned assumption of a new channel for ultrafast ISC connected with a higher-lying excited singlet state within the  $S_1$  manifold is correct, we have to observe a delayed rise of the ESA at 600 nm as well as a fast rise in the region of TTA at 460 nm. The corresponding kinetics is shown in Fig. 8. Indeed, we observe that the maximum of the ESA is delayed by about 5 ps relative to the excitation pulse (Fig. 8a). The time constants for the shown bi-exponential fit, which consists of a superposition of decaying and rising contributions, are  $(3.5 \pm 1.4) \text{ ps}$  and  $(165 \pm 6) \text{ ps}$ . The fit was performed at  $\lambda = 680 \text{ nm}$  to obtain the undisturbed ESA kinetics, because the maximum of the ESA at  $\lambda = 600 \text{ nm}$  is partially overlapped by TTA. The situation for the TTA

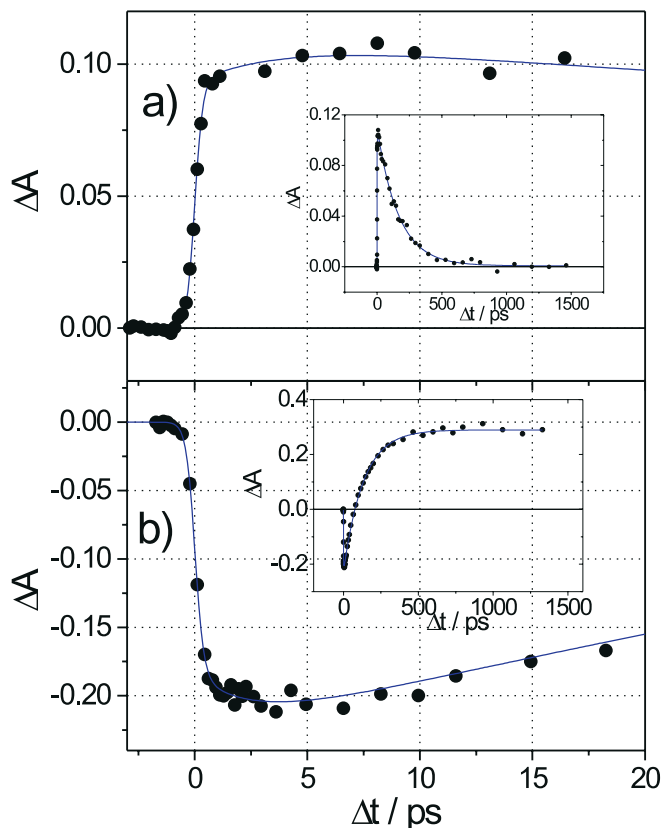


**Fig. 8a,b.** Time dependence of  $\Delta A$  for 3T pumped at 375 nm and probed at **a** 680 nm showing the delayed rise of ESA (bi-exponential fit yields  $\tau_1 = 3.5 \text{ ps} \pm 1.4 \text{ ps}$  and  $\tau_2 = 165 \text{ ps} \pm 6 \text{ ps}$ ); and **b** 460 nm showing the delayed TTA/fluorescence (bi-exponential fit yields  $\tau_1 = 2.3 \text{ ps} \pm 0.8 \text{ ps}$  and  $\tau_2 = 133 \text{ ps} \pm 7 \text{ ps}$ )

(Fig. 8b) is more complicated, but yields essentially the same results: because of the overlap of TTA and fluorescence the absorbance change  $\Delta A$  at 460 nm reflects only for long delay times the undisturbed TTA, whereas at short delay times we observe negative  $\Delta A$  values due to fluorescence. Nevertheless, the delayed (negative) maximum in the kinetics at 5 ps can be interpreted as a fast-rising component of TTA and/or fluorescence during the first picoseconds. It can be fitted well with the same bi-exponential function as used for fitting the kinetics of the ESA with decaying and rising contributions. The resulting time constants amount to  $2.3 \text{ ps} \pm 0.8 \text{ ps}$  and  $133 \text{ ps} \pm 7 \text{ ps}$ . Within the statistical error the short time constant is in very good agreement with the parameters obtained from fitting the kinetics of the ESA. The long time component is probably falsified by the overlapping fluorescence.

### 3 Discussion

The aim was to study the connection between the formation kinetics and the high triplet quantum yields of 2T and 3T.

In 3T we found triplet formation and quantum yield to be dependent on the excitation energy in a one-photon absorption process. Whereas at excitation at the band gap (0-0 transition) with  $\lambda = 400 \text{ nm}$  the decay is determined by the fluorescence lifetime of  $S_1$  (165 ps [12]), with increasing excitation energy ( $\lambda = 381 \text{ nm}$ ) an additional fast channel for

triplet formation with a time constant of about 2 ps becomes more dominant. Our measurements in the bleaching region (Fig. 5 and [9]) as well as the examination of excitation-energy dependence on the time-resolved spectra (Figs. 6,7) allow us to fix the energetic position of the second starting level for ISC at 3.26 eV (381 nm). The low difference of only 0.21 eV above the lowest excited singlet state  $S_1$  excludes a higher electronic excited state  $S_n$ , because in this case the relaxation would have to proceed much faster than the observed ISC with 2 ps. On the other hand, ‘pure’ intramolecular vibrational relaxation at large molecules takes place on a time scale of only 100–200 fs. Therefore, we suppose that we found an intermediate state which is populated by molecules in a non-relaxed conformation. Our laser pulse excites molecules with randomly twisted monomer units in the non-planar ground state up to the  $S_1$  manifold. Because of its short pulse duration it transfers the ground-state geometry to the excited state. As is known from fluorescence spectra [8] and theoretical calculations [13], the relaxed excited state should exhibit a quinoid-like, planar structure. Therefore, we interpret the short time constant of 2 ps derived from one-colour experiments (Fig. 5) as well as from spectrally resolved kinetics (Fig. 8a,b) as the time constant for the planarisation process following photo-excitation. On this time scale a second channel for fast intersystem crossing is opened (Fig. 9a). The effectiveness is enhanced by the close energetic neighbourhood of the  $T_2$  state located at almost the same energy, as was shown previously [1]. Further confirmation for our assumption of conformational changes comes from recent work on 4T [14], where a planarisation process within a time of 4 ps was found. Additionally, theoretical studies have been reported for 3T [13], where the dependence of the energy of ground and excited states on the twisting angles between the thiophene rings was shown. According to these calculations one should expect at room temperature a distribution of the angles between the twisted thiophene rings around the equilibrium angle of  $30^\circ$  in the ground state, while the energetic minimum of the excited-state potential curve would be located at an angle of  $0^\circ$ .

We also examined the mechanism of triplet formation in dependence on excitation intensity at different wavelengths. From the results we concluded that at excitation energies higher than the intermediate state at 3.26 eV, triplets were populated via ISC from the lowest as well as the twisted  $S_1$  state, whereas we observed a contribution via two-photon absorption when exciting with higher pump intensities and energies not sufficient to excite the twisted state at 381 nm [15].

For the studies on 2T we used two-photon absorption at  $\lambda_{\text{pump}} = 375 \text{ nm}$  for excitation. In this way a level high above the 0-0 transition was excited.

Examining the transient spectra in Fig. 2, the first question after assignment of ESA (500 nm) and TTA/fluorescence (426 nm) arises regarding the reason for the band around  $\lambda = 590 \text{ nm}$ . This band was not observed in experiments using one-photon excitation at  $\lambda = 308 \text{ nm}$  [10]. From ns experiments [16], however, it is known that two radical cation absorption bands which have their maxima at 420 nm and at 590 nm can be observed if 2T is dissolved in a mixture of acetonitrile and tetracyanoethylene (TCNE), which acts as an efficient electron acceptor. In contrast, in our experiments the sample molecules are excited with two photons having an en-

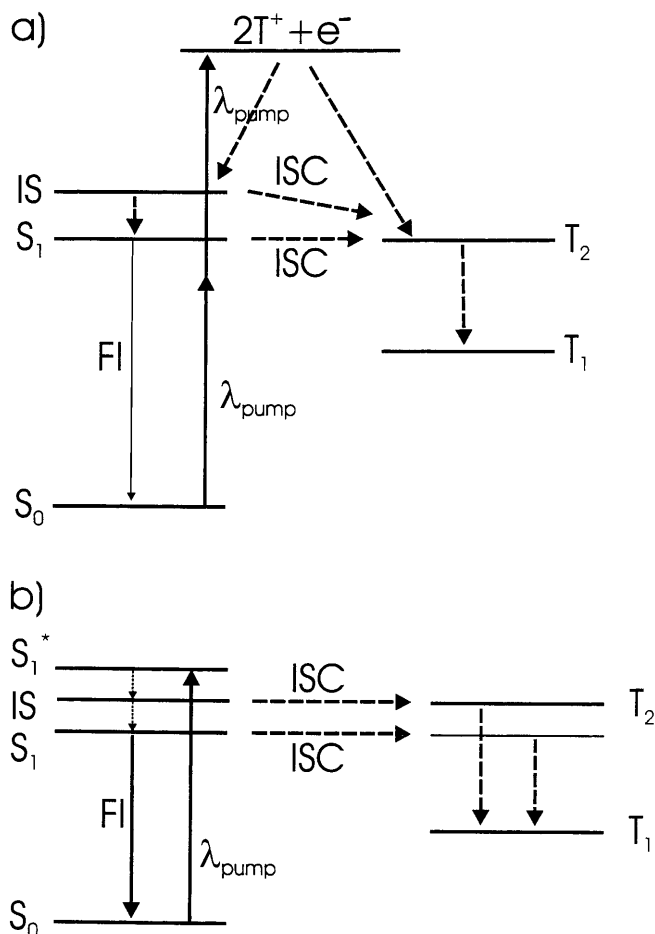


**Fig. 9a,b.** Schematic energy-level schemes proposed for explaining the observed kinetics for 2T (a) and 3T (b). IS denotes the intermediate state, which represents a non-relaxed geometry described in the text. In the case of 2T  $\lambda_{\text{pump}} = 375$  nm, while it was variable for 3T measurements. The unlabelled state in b corresponds to a vibrational level within the  $T_1$  manifold

ergy of 3.31 eV each, so we offer enough energy for radical cation formation.

We used pure ethanol as solvent, which does not act to the same extent as an electron acceptor as TCNE, so it seems reasonable to attribute the observed decay time of the radical cation absorption band ( $\tau = 62 \text{ ps} \pm 9 \text{ ps}$ , Fig. 4a) to geminate recombination of radical cations and the electron, which in ethanol does not manage to escape from the positive ion. Because of the fact that there exist no symmetry selection rules for recombination and therefore the formation of triplets is preferred, we think that the observed rise of the TTA on the same time scale ( $\tau = 58 \text{ ps} \pm 18 \text{ ps}$ , Fig. 4b) also reflects the process of recombination of radical cations. The formation of radicals would be another reason for the very complicated kinetics on the short time scale at 426 nm (Fig. 4b,  $\Delta t < 75 \text{ ps}$ ), because the second known radical absorption band – showing an even higher extinction coefficient – has its maximum at 420 nm [16]. This leads for short time delays to an overlap of fluorescence (decaying within 30–50 ps), TTA (fast-rising component of about 1.4 ps and ‘normal’ component of 58 ps) and radical absorption (decaying within 62 ps). Moreover, it is probable that we also see a contribution of a cross-correlation peak of pump and probe beams, previously observed in one-

colour experiments with  $\lambda_{\text{pump}} = \lambda_{\text{probe}} = 400 \text{ nm}$  [17]; it would be more intense than effects arising from two-photon excitation.

The decay of the ESA (Fig. 3) was found to show two time constants, 1.4 ps and 29.6 ps. 2T exists in two conformers in the ground state [8, 18]. The most simple explanation for the two time constants is to interpret them as time constants of the trans- and the cis-conformer. But the energy difference of these conformers is very small in  $S_1$  (and also in  $S_0$ ), so that we do not think that such strongly different decay times are possible.

Having in mind our model for the fast intersystem crossing in 3T explained above, one more reasonable process could be geometrical relaxation, which also has to occur in 2T because both theoretical calculations [18] and experimental results from gas-phase experiments [19] indicate an angle of 30–35° between the thiophene monomer units in the ground state, while the atomic-charge distribution of the excited state exhibits the planar quinoid-like structure, too [8]. The electronic absorption processes (both for one- and two-photon absorption) proceed in a time scale of  $10^{-15} \text{ s}$  for a single molecule. That means that the positions of the nuclear coordinates remain fixed during the excitation (this seems to be the case even during the energy relaxation to  $S_1$ ). Therefore, it may be that we observe processes from an unrelaxed as well as an already relaxed excited state. In this case the following planarisation would take place in 1.4 ps. During this process single and double bonds change their positions; especially, the inter-ring bonds alter from single to double bonds, like in 3T. The  $S_1$  state becomes planar and rigid. In this way the kinetics at 500 nm would be explained as a superposition of the ESA of the (lowest)  $S_1$  state and a second one arising from the non-planar, unrelaxed conformer, which undergoes preferably fast ISC and therefore leads to a fast decay in the ESA kinetics (Fig. 9b). Perhaps we have to consider the re-orientation of the first solvent shell to the relaxed geometry, which may slow down the entire process. The solvent effect depends on the dipole-moment change between  $S_0$  and  $S_1$ . This change is zero for 2T but significant for 3T.

On the other hand we have to keep in mind that – in contrast to the measurements of 3T – we use two-photon excitation. As a result, during the relaxation a large manifold of singlet states, and likewise (if we admit ISC from higher singlet states) a large number of triplet states can be populated. Because little is known about these states, we cannot exclude additional influence of ESA from these highly excited singlet or triplet states.

In conclusion, our hypothesis is that triplet formation takes place during the geometry relaxation. In the case of 3T we could observe the slightly delayed arising ESA and TTA spectrum (see Fig. 8a,b) and it was possible to determine the energetic position of the associated intermediate state within the  $S_1$  manifold. In 2T we see only two different decays of the ESA spectrum (Fig. 3). The fast decay can be described by geometrical relaxation, which proceeds in parallel with triplet formation. The slow component describes the ‘normal’  $S_1$  depopulation already observed by others [8, 10, 11]. Furthermore a radical cation absorption band was detected decaying on the same time scale as the TTA rises.

From the experimental fact that we observe the effects of these processes in the ESA spectra, we conclude that the primary processes proceed in the singlet manifold. That means



that even in the case of very high triplet quantum yields and strong energy resonance between  $S_1$  and  $T_2$  the intersystem crossing follows after the singlet processes.

*Acknowledgements.* The authors are grateful to the Deutsche Forschungsgemeinschaft for providing financial support within the Schwerpunktprojekt "Fs-Spektroskopie elementarer Anregungen in Atomen, Molekülen und Clustern".

## References

1. S. Rentsch, J.-P. Yang, W. Paa, E. Birckner, J. Schiedt, R. Weinkauff: *Phys. Chem. Chem. Phys.* **1**, 1707 (1999)
2. D. Fichou (Ed.): *Handbook of Oligothiophenes* (VCH-Verlag, Weinheim 1999)
3. R.A.J. Janssen: In *Primary Photoexcitations in Conjugated Polymers: Molecular Exciton versus Semiconductor Band Model*, ed. by N.S. Sariciftci (World Scientific, Singapore 1997)
4. G. Gigli, G. Barbarella, L. Favaretto, F. Cacialli, R. Cingolani: *Appl. Phys. Lett.* **75**(4), 439 (1999)
5. G. Barbarella, L. Favaretto, G. Sotgiu, M. Zambianchi, V. Fattori, M. Cocchi, F. Cacialli, G. Gigli, R. Cingolani: *Adv. Mat.* **11**(16), 1375 (1999)
6. H. Chosrovian, S. Rentsch, D. Grebner, D.U. Dahm, E. Birckner: *Synth. Met.* **60**, 23 (1995)
7. J.R. Sheats, H. Antoniadis, M. Hueschen, W. Leonard, J. Miller, R. Moon, D. Roitman, A. Stocking: *Science* **273**, 884 (1996)
8. R.S. Becker, J. Seixas de Melo, A.L. Macanita, F. Elisei: *J. Phys. Chem.* **100**, 16 683 (1996)
9. W. Paa, J.-P. Yang, M. Helbig, J. Hein, S. Rentsch: *Chem. Phys. Lett.* **292**, 607 (1998)
10. D. Grebner, M. Helbig, S. Rentsch: *J. Phys. Chem.* **99**, 16991 (1995)
11. P. Emele, D.U. Meyer, N. Holl, H. Port, H.C. Wolf, F. Würthner, P. Bäuerle, F. Effenberger: *Chem. Phys.* **181**, 417 (1994)
12. A. Yang, S. Hughes, M. Kuroda, Y. Shiraishi, T. Kobayashi: *Chem. Phys. Lett.* **280**, 475 (1997)
13. N. DiCésare, M. Belletête, A. Donat-Bouillud, M. Leclerc, G. Durocher: *J. Luminescence* **81**, 111 (1999)
14. G. Lanzani, M. Nisoli, S. De Silvestri, R. Tubino: *Chem. Phys. Lett.* **251**, 339 (1996)
15. J.-P. Yang, W. Paa, S. Rentsch: *Chem. Phys. Lett.* **320**, 665 (2000)
16. C.H. Evans, J.C. Scaiano: *J. Am. Chem. Soc.* **112**, 2694 (1990)
17. W. Paa, J.-P. Yang, S. Rentsch: CLEO/EUROPE-EQEC'98, Glasgow, Scotland, QTuG69
18. N. DiCésare, M. Belletête, F. Raymond, M. Leclerc, G. Durocher: *J. Phys. Chem. A* **101**, 776 (1997)
19. A. Almenningen, O. Bastiansen, P. Svendsas: *Acta Chem. Scand.* **12**, 1671 (1958)